

1 **Prenatal hyperandrogenism induces alterations that affect liver lipid metabolism**

2 Giselle Adriana Abruzzese^{1*}, Maria Florencia Heber¹, Silvana Rocio Ferreira¹, Leandro
3 Martin Velez¹, Roxana Reynoso², Omar Pedro Pignataro³, Alicia Beatriz Motta¹

4 ¹ Laboratorio de Fisiopatología Ovárica, Centro de Estudios Farmacológicos y Botánicos,
5 Universidad de Buenos Aires (UBA), Consejo Nacional de Investigaciones Científicas y
6 Técnicas (CONICET), Buenos Aires, Argentina

7 ² Laboratorio de Endocrinología, Departamento de Fisiología, Facultad de Medicina,
8 Universidad de Buenos Aires (UBA), Argentina

9 ³ Laboratorio de Endocrinología Molecular y Transducción de Señales, Instituto de Biología y
10 Medicina Experimental, Consejo Nacional de Investigaciones Científicas y Técnicas
11 (CONICET), Universidad de Buenos Aires (UBA), Buenos Aires, Argentina

12

13 ***Corresponding author:** Giselle A. Abruzzese. Paraguay 2155 17th floor CP1121, CEFYBO-
14 FMED-UBA, Buenos Aires, Argentina. giselleabruzzo@gmail.com . 45083680 int. 217.

15

16 **Short title:** Androgen excess alters liver lipid metabolism

17 **Keywords:** polycystic ovary syndrome, fatty liver, prenatal hyperandrogenism, lipid
18 metabolism

19 **Word count:** 4718

20

21

22

23

24 Abstract

25 Prenatal hyperandrogenism is hypothesized as one of the main factors contributing to
26 the development of polycystic ovary syndrome (PCOS). PCOS patients have high risk
27 of developing fatty liver and steatosis. This study aimed to evaluate the role of prenatal
28 hyperandrogenism in liver lipid metabolism and fatty liver development. Pregnant rats
29 were hyperandrogenized with testosterone. At pubertal age, the prenatally
30 hyperandrogenized (PH) female offspring displayed both ovulatory (PHov) and
31 anovulatory (PHanov) phenotypes that mimic human PCOS features. We evaluated
32 hepatic transferases, liver lipid content, the balance between lipogenesis and fatty acid
33 oxidation pathway, oxidant/antioxidant balance and pro-inflammatory status. We also
34 evaluated the general metabolic status through growth rate curve, basal glucose and
35 insulin levels, glucose tolerance test, HOMA-IR index and serum lipid profile.
36 Although neither PH group showed signs of liver lipid content, the lipogenesis and fatty
37 oxidation pathways were altered. The PH groups also showed impaired
38 oxidant/antioxidant balance, a decrease in the pro-inflammatory pathway (measured by
39 prostaglandin E2 and cyclooxygenase-2 levels), decreased glucose tolerance, imbalance
40 of circulating lipids and increased risk of metabolic syndrome. We conclude that
41 prenatal hyperandrogenism generates both PHov and PHanov phenotypes with signs of
42 liver alterations, imbalance in lipid metabolism and increased risk of developing
43 metabolic syndrome. The anovulatory phenotype showed more alterations in liver
44 lipogenesis and a more impaired balance of insulin and glucose metabolism, being more
45 susceptible to the development of steatosis.

46

47

48 **Introduction**

49 Polycystic ovary syndrome (PCOS) is one of the most common endocrine and
50 metabolic disorders that affect women in their reproductive age (Franks 2003) and its
51 clinical manifestations often emerge during puberty (Rosenfield 2007; Yan, et al. 2013).
52 PCOS etiology remains controversial and current theories emphasize on genetic and
53 intrauterine origins coupled with environmental factors such as the diet and altered
54 lifestyle patterns (Franks 1995). It has been reported that prenatal androgen exposure is
55 able to induce polycystic ovaries in rats (Demissie, et al. 2008; Foecking, et al. 2008),
56 monkeys (Abbott, et al. 2010) and sheep (Manikkam, et al. 2006) and that fetal
57 programming, mediated by prenatal hyperandrogenism, is related to hyperinsulinemia,
58 dyslipidemia, insulin resistance (IR), cardiovascular disease and metabolic syndrome
59 (Amalfi, et al. 2012; Demissie et al. 2008; Heber, et al. 2013). However, how fetal
60 programming impacts on different tissues is unknown.

61 The liver is involved in lipid synthesis, transportation and storage, as well as in glucose
62 and insulin metabolism (Paschos and Paletas 2009), all key factors in PCOS
63 pathogenesis (Baranova, et al. 2011; den Boer, et al. 2004; Paschos and Paletas 2009;
64 Vassilatou 2014). One of the most frequent hepatic affections, related to metabolic
65 abnormalities, is non-alcoholic fatty liver disease (NAFLD), which affects 20%-30% of
66 the general population (Vassilatou 2014). NAFLD includes a clinicopathologic
67 spectrum of conditions that encompass from simple steatosis (triglyceride (TG)
68 accumulation in hepatocytes) to steatohepatitis with inflammation, fibrosis and even
69 cirrhosis (Browning and Horton 2004). NAFLD pathogenesis remains unknown and
70 there are many hypotheses about its origin (Lee, et al. 2014; Yasui, et al. 2012).
71 Currently, the most accepted model proposes a multiple and parallel hits hypothesis.

72 Fatty acids and their metabolites are the lipotoxic agents involved in NAFLD
73 development (Day and James 1998; Lin, et al. 2014), being the increase in oxidative
74 stress one of the key factors in NAFLD pathogenesis (Lin et al. 2014; Madan, et al.
75 2006).

76 In physiological conditions, in the liver, there is an equilibrium between the uptake and
77 exportation of fatty acids (which in turn can be esterified or to be oxidized) (Browning
78 and Horton 2004; Kawano and Cohen 2013). However, when the balance between
79 lipolysis and lipogenesis is altered, or fatty acid influx to the liver is increased, lipid
80 droplets could accumulate in the liver, leading to steatosis and even NAFLD (den Boer
81 et al. 2004; Kawano and Cohen 2013).

82 A common feature of NAFLD and PCOS is IR (Gambarin-Gelwan, et al. 2007;
83 Schwimmer, et al. 2005). However, it remains controversial whether IR is the key cause
84 in the development of NAFLD in women with PCOS (Gambarin-Gelwan et al. 2007;
85 Liang and Ward 2006). Since PCOS patients with hyperandrogenic phenotypes have a
86 higher prevalence of developing NAFLD, it has been suggested that androgens could
87 contribute to the development of the pathology (Vassilatou 2014; Vassilatou, et al.
88 2010). We have previously demonstrated that the levels of androgen administered in
89 pregnant rats are directly related to the PCOS-like phenotype displayed in the female
90 offspring during the pubertal age (Amalfi et al. 2012) and that the fetal programming
91 generated by androgens leads to metabolic alterations, particularly in lipid metabolism,
92 which worsen through life (Heber et al. 2013).

93 Based on the above, the aim of this study was to evaluate the effect of prenatal
94 hyperandrogenism on the liver function and lipid metabolism.

95

96 **Materials and methods**

97 **Animals and treatments**

98 Virgin female rats of the Sprague Dawley strain were mated with fertile males of the
99 same strain. Three females and one male were housed in each cage under controlled
100 conditions of light (12 h light, 12 h dark) and temperature (23-25 °C). Animals received
101 food and water *ad libitum*. Day 1 of pregnancy was defined as the morning on which
102 spermatozoa were observed in the vaginal fluid. As previously described (Demissie et
103 al. 2008), pregnant rats (N=15) received subcutaneous injections of 1 mg of free
104 testosterone (T-1500; Sigma, St. Louis, MO, USA) dissolved in 100 µl sesame oil from
105 day 16 to day 19 of pregnancy. This hormonal paradigm mimics the fetal testosterone
106 surge that is observed in male rats when the reproductive axis in the fetus is established.
107 Another group (N=15) received only 100 µl of sesame oil. The dose was selected based
108 on previous findings of our lab (data not published) and other studies which have shown
109 that this dose leads to ovulatory and anovulatory phenotypes and that higher doses lead
110 only to anovulatory phenotypes during the adult life and even to vaginal atresia (Wolf,
111 et al. 2002). Under the conditions of our animal facilities, spontaneous term labor
112 occurs on day 22 of gestation. Female offspring were separated from males at 21 days
113 of age and sacrificed during pubertal age at 60 days of age. Those from
114 hyperandrogenized mothers were the prenatally hyperandrogenized (PH) group and
115 those from mothers injected with sesame oil were the control (Ctl) group. Animals were
116 allowed free access to Purina rat chow (Cooperación SRL, Argentina) and water. All the
117 procedures involving animals were conducted in accordance with the Animal Care and
118 Use Committee of Consejo Nacional de Investigaciones Científicas y Técnicas
119 (CONICET) 1996, Argentina, and the study was approved by the Ethics Committee of

120 the School of Medicine of University of Buenos Aires. To establish the phenotype
121 diversity, the above procedures were independently repeated three times.

122 At 60 days of age, 75 female offspring from each group were anesthetized with carbon
123 dioxide and killed by decapitation. Trunk blood was collected and serum was separated
124 and kept at -80°C for further studies. Ovaries and liver were extracted and conserved at
125 -80°C or fixed in 4% (v/v) formaldehyde for histological studies. All animals were
126 randomly assigned for each assay.

127 **Characterization of the prenatally hyperandrogenized murine model**

128 Serum testosterone was quantified from 15 offspring from each group by
129 radioimmunoassay (RIA) as previously described (Amalfi et al. 2012). Serum estradiol
130 levels were quantified by Cobase immunoassay analyzers using an Electro
131 Chemiluminescence Immuno Assay (ECLIA) following the manufacturer's instructions.
132 The intra- and interassay coefficients of variation (CVs) were 7.3% and 13.2%
133 respectively for testosterone and 3.93% and 7.08% respectively for estradiol.

134 The estrous cycle was determined by vaginal smears taken daily from 45 to 60 days of
135 age in all the animals.

136 Regular ovulatory animals were those that showed smears displaying the four stages of
137 the estrous cycle in the following order: proestrus, estrus, metaestrus, diestrus, with
138 cycles of 4 to 6 days. Irregular ovulatory animals were both those that showed some
139 smears displaying an estrous stage but further smears not following the progress of the
140 cycle as described above, and those whose cycles lasted 7 days or more (PHov).
141 Anovulatory animals were whose smears showed metaestrus, diestrus, or a combination
142 of both for four consecutive days, and were thus considered to be non-cycling (PHanov)
143 (Karim, et al. 2003).

144 To evaluate ovarian histology, 10 ovaries from each group were removed and
145 immediately fixed in 4% (v/v) formaldehyde and analyzed by two different
146 investigators. Ovaries were embedded in paraffin wax and consecutively cut. To prevent
147 counting the same follicle twice, 6- μ m step sections were mounted at 50- μ m intervals
148 onto microscope slides. Then, slides were stained with hematoxylin and eosin
149 (Woodruff, et al. 1990).

150 **Hepatic enzymes**

151 Serum levels of alanine aminotransferase (ALT), aspartate aminotransferase (AST) and
152 gamma-glutamyl transferase (GGT) were quantified by colorimetric enzymatic methods
153 (Wiener Lab, Argentina) following the manufacturer's instructions. The chromophoric
154 products were measured at 340 nm for ALT and AST and at 405 nm for GGT, all at
155 25°C. The intra- and interassay Cvs were 3.02% and 5.63% for ALT, 4.4% and 4.9%
156 for AST, and 1.62% and 5% for GGT.

157 **Liver lipid and TG content**

158 Fragments of hepatic tissue randomly selected from 15 female offspring from each
159 group were fixed in formaldehyde 4% (v/v), cut in cryostat and stained with SUDAN IV
160 to visualize lipid droplets using hematoxylin as contrast stain. The intestine of tadpole
161 was used as a positive control of the SUDAN IV technique (Regueira, et al. 2016). To
162 evaluate the TG content in the liver, 15 frozen samples of each group were saponified
163 and TG content was quantified by comparing to a glycerol standard curve by a
164 commercial kit (Wiener Lab, Argentina), as previously described (Chow, et al. 2011).

165 **Hepatic lipid metabolism**

166 The mRNA expression of Acetyl-CoA carboxylase (ACC) 1 and2 (*Acaca* and *Acacb*,
167 respectively), Fatty acid Synthase (*Fas*), stearyl-CoA desaturase (*Scd1*), Sterol

168 regulatory element-binding protein1 (*Srebp1*), carbohydrate response element binding
169 protein (*Chrebp*), Peroxisome proliferator-activated receptor alpha and gamma
170 (*Pparalpha* and *Ppargamma*) and PPARgamma co-activator 1alpha (*Pgc1a*) was
171 evaluated by Real-Time PCR analysis in 15 different samples from each group. Total
172 mRNA from hepatic tissue was extracted using RNAzol RT (MRC gene, Molecular
173 Research Center, Cincinnati, OH, USA) following the manufacturer's instructions.
174 cDNA was synthesized from 500 ng mRNA by using random primers. Real-Time PCR
175 analysis was performed from this cDNA by means of the real mix B124-100
176 (Biodynamics SRL, USA). The amplified products were quantified by fluorescence
177 using the Rotor Gene 6000 Corbett and mRNA abundance was normalized to the 60s
178 Ribosomal protein L32 (*L32*) amount. L32 was validated as a reference gene because
179 the variance between treatments did not differ. Results are expressed as arbitrary units.
180 The primers are shown in Table 1.

181 **Liver oxidant/antioxidant balance**

182 The oxidant–antioxidant balance in liver tissue was evaluated as the lipid peroxidation
183 index and the content of the antioxidant glutathione (GSH) in 15 samples of each group.
184 The amount of malondialdehyde formed from the breakdown of polyunsaturated fatty
185 acids is taken as an index of the peroxidation reaction. The method used in this study
186 was as that previously described (Amalfi et al. 2012; Heber et al. 2013). The reduced
187 form of GSH, which comprises the bulk of cellular protein sulfhydryl groups, was
188 quantified as previously described (Amalfi et al. 2012; Heber et al. 2013).

189 **Liver inflammatory status**

190 The inflammatory status in liver tissue was measured by evaluating the levels of
191 Prostaglandin E (PGE) and cyclooxygenase-2 (COX2), the limiting enzyme of its

192 synthesis. PGE was determined by RIA as previously reported (Motta, et al. 1999).
193 COX2 was measured by the Western blotting technique, using 200 mg of liver tissue
194 from 10 independent samples per group, as previously described (Amalfi et al. 2012).

195 **General metabolism imbalance**

196 The body weight of all the animals of all the groups was determined at 21, 28, 38, 45
197 and 60 days of age.

198 Basal insulin levels were measured by an ELISA kit, following the manufacturer's
199 instructions (Abcam Insulin Human ELISA Kit) and basal glucose levels were
200 quantified by colorimetric enzymatic methods (Wiener Lab, Argentina) (N=10 per
201 group). The intra- and interassay Cvs were 10% and 12% respectively for insulin and
202 1.39% and 1.92% respectively for glucose.

203 The glucose tolerance test (IPGTT) was performed in separate groups of ten female
204 offspring from each group, as previously described (Amalfi et al. 2012; Demissie et al.
205 2008). The homeostatic model assessment for IR (HOMA-IR) was determined (Yan et
206 al. 2013). The circulating lipid profile was evaluated as previously described and the
207 TG/HDL cholesterol ratio was taken as a marker of metabolic syndrome risk (Heber et
208 al. 2013).

209 **Statistical analysis**

210 Statistical analyses were carried out using the Instant program (GraphPad software, San
211 Diego, CA, USA). ANOVA with post-hoc Tukey test was used to compare the three
212 treatments. Statistical significance was considered as $p < 0.05$.

213

214

215

216 **Results**

217 **Characterization of the prenatally hyperandrogenized murine model**

218 The PHov and PHanov groups showed higher serum testosterone levels than the control
219 group, but only PHanov animals displayed lower estradiol levels than the control (Fig.
220 1A and 1B, $p < 0.01$). Figure 1C shows a representative ovarian tissue section from the
221 control group. The general appearance of the tissue resembled normal histology: a
222 central medulla consisting mainly of fibromuscular stroma and corpora lutea and antral
223 follicles located in the peripheral cortex. Histological examination of ovaries from the
224 PHov and PHanov groups (Fig. 1C and 1D) revealed the presence of corpora lutea,
225 cysts and an excess of small antral follicles. In addition, in PHanov animals, the ovary
226 was disorganized as compared to the control group and small follicles could be seen
227 invading the central medulla. The detail in figure 1E shows that cysts present a layer of
228 theca cells and a thin compacted formation of granulosa cells.

229 Regarding the estrous cycle, in the three independent repetitions of the animal
230 procedure, always 100% of the control rats showed a regular estrous cycle. Within the
231 PH group, 43-51% showed irregular estrous cycles and were considered as PHov,
232 whereas 27-39% presented anovulatory cycles and were considered PHanov.
233 Testosterone did not affect the age of vaginal opening.

234 **Prenatal hyperandrogenism and hepatic alterations**

235 ALT levels were increased in the PHov group (Fig. 2A, $p < 0.01$). Neither AST or GGT
236 levels were affected in the PHov or PHanov groups as compared with the control group
237 (Fig. 2B and 2C respectively, $p > 0.05$).

238 As compared with the positive control of the SUDAN IV technique (Fig. 2D, arrows),
239 neither the control group (Fig. 2E) nor the PHov or PHanov phenotypes (Fig. 2F and

240 2G) showed hepatic lipid droplets. In addition, no differences were found in the hepatic
241 TG content between groups (Fig. 2H, $p>0.05$).

242 Regarding the transcription factors that are mediators of lipogenesis, we found that
243 *Ppargamma* and *Srebp* mRNA levels were higher in both PH groups than in the control
244 group (Fig. 3A and 3B, $p<0.05$), whereas *Chrebp* levels were only altered in the
245 PHanov animals (Fig. 3C, $p<0.05$). Regarding the enzymes involved in lipogenesis, we
246 found that the mRNA levels of the genes encoding both isoforms of Acetyl-CoA
247 carboxylase (*Acaca* and *Acacb*) were decreased in both PH groups (Fig. 3D and 3E,
248 $p<0.05$). *Fas* mRNA levels were increased in the PH groups (Fig. 3F, $p<0.05$), whereas
249 *Scd1* mRNA levels were only impaired in PHanov animals (Fig. 3G, $p<0.05$).

250 Regarding fatty acid oxidation pathways, we found that *Pparalpha* mRNA levels
251 showed no differences between the control and PHov groups but were decreased in
252 PHanov (Fig. 3H, $p<0.01$), and that *Pgc1a* levels were lower in both PH animals than in
253 controls (Fig. 3I, $p<0.01$).

254 *L32* was validated as a reference gene, obtaining no statistical difference in the stability
255 between treatments measured by the Ct (threshold cycle) (control= $21.76 + 0.24$; PHov=
256 $21.36 + 0.30$; PHanov= $21.70 + 0.34$; $p=0.67$).

257 The lipid peroxidation index was higher in the PH groups than in the control (Fig. 4A,
258 $p<0.05$). GSH levels were altered in both PH groups as compared to the control. GSH
259 levels were increased in the PHov groups and decreased in the PHanov group (Fig. 4B,
260 $p<0.01$).

261 Both the levels of PGE and the protein expression of COX2 were lower in the PH
262 groups than in the control group. In addition, the PGE levels were lower in the PHanov
263 group than in the PHov animals (Fig. 4C and 4D, $p<0.01$).

264 **Prenatal hyperandrogenism and metabolic derangements**

265 Prenatal hyperandrogenism did not affect the body weight from prepubertal to pubertal
266 age (Fig. 5A, $p=0.41$). Insulin levels were increased in both PH groups as respect to
267 controls (Fig. 5B, $p<0.05$), and basal glucose levels were impaired in the PHanov group
268 (Fig. 5C, $p<0.05$). The IPGTT showed that prenatal hyperandrogenism induced
269 increased levels of circulating glucose (Fig. 5D), represented by the area under the
270 curve of glucose concentration (control = 14873.0 ± 119.7 ; PHov = 21045.0 ± 164.0 ;
271 PHanov= 2090.0 ± 156.6 in arbitrary units, control vs. PHov $p<0.01$; control vs.
272 PHanov $p<0.05$; PHov vs. PHanov $p>0.05$). The HOMA-IR index was increased in the
273 PHanov group as compared to controls (Fig. 5E, $p<0.05$).

274 Both PH groups showed an altered circulating lipid profile, displaying higher levels of
275 circulating low-density lipoprotein cholesterol (LDL) (Fig. 6A, $p<0.05$) and TG than the
276 control group (Fig. 6B, $p<0.01$). No significant differences were found in the levels of
277 total cholesterol or high-density lipoprotein (HDL) cholesterol (Fig. 6C and 6D,
278 $p>0.05$). The TG/HDL cholesterol ratio, as a marker of metabolic syndrome risk was
279 higher in both PH groups than in the control group (control= 1.13 ± 0.34 ; PHov= $2.42 \pm$
280 0.24 ; PHanov= 2.65 ± 0.39 , $p<0.05$; PHov vs. control and PHanov vs. control, $p>0.05$
281 PHov vs. PHanov).

282

283 **Discussion**

284 The developmental origins of PCOS are controversial. Some authors have reported that
285 an altered *in utero* environment could be responsible for metabolic diseases and PCOS
286 features development in different species (Abbott, et al. 2005; Demissie et al. 2008;
287 Hogg, et al. 2011), whereas others propose PCOS as a multiplicity of etiologies and not

288 a simple mechanism and emphasize genotype features (Franks and Berga 2012;
289 Gluckman and Hanson 2004). It is known that both the embryo development stages and
290 early postnatal life period are crucial to condition adult health life. Thus, currently used
291 PCOS animal models focus on these critical development time windows (Abbott et al.
292 2010; Amalfi et al. 2012; Demissie et al. 2008; Jang, et al. 2015; Manikkam et al.
293 2006). Furthermore, the metabolic and endocrine alterations found in the prenatal
294 models lead to several long-term effects, thus highlighting the importance of the *in*
295 *utero* environment.

296 In the present study, we reproduced a murine model wich displayed PCOS features
297 leading to two phenotypes: both with hyperandrogenism and ovarian alterations, such as
298 an increase in the number of preantral follicles and the formation of cysts. Nearly 50%
299 of the cases of the PH group presented irregular ovulatory estrous cycles whereas
300 around 40% of the cases in PH group presented the anovulatory phenotype.

301 Ovaries from PCOS women are known to contain an increased number of small follicles
302 that have and excessive early growth but with follicular arrest, thus preventing the
303 selection and further maturation of a dominant follicle. These data are in accordance
304 with our results showing that androgens play a role in follicle recruitment (Jonard and
305 Dewailly 2004).

306 We found that PH rats showed incipient liver damage. These data are in agreement with
307 previous reports that suggest that the intrauterine environment plays an important role in
308 the development of both NAFLD and PCOS during postnatal life (Baranova, et al.
309 2013; Brumbaugh and Friedman 2014).

310 Contrary to other reports (Demissie et al. 2008; Hogg et al. 2011), we found no lipid
311 accumulation in the liver. This difference could be due to the higher doses of androgens

312 used in those reports and is in agreement with our previous findings where higher doses
313 of androgens induced a more severe PCOS-like phenotype as well as worse endocrine
314 and metabolic disturbances (Amalfi et al. 2012). To deepen the study of lipid
315 metabolism in the liver, we evaluated the status of the *de novo lipogenesis* pathway and
316 β -fatty acid oxidation mediators (Figure 7). To assess the lipogenic pathway, we
317 evaluated the role of three transcription factors involved in the regulation of *de novo*
318 lipogenesis. Two of them, *Srebp* and *Chrebp*, are regulated by insulin and glucose
319 levels, respectively, and both regulate the expression of genes encoding lipogenic
320 enzymes (Browning and Horton 2004; Strable and Ntambi 2010). Our results showed
321 that the PH groups presented high levels of *Srebp*, consistent with the high levels of
322 serum insulin found in PH animals. Moreover, *Chrebp* was impaired in the PHanov
323 group, showing a correlation with basal glucose levels in those animals. These data are
324 in accordance with that described by other authors showing that in the hyperinsulinemic
325 and even more in the IR states, SREBP1-c transcription is stimulated and could lead to
326 *de novo* fatty acid synthesis (Browning and Horton 2004; Strable and Ntambi 2010).
327 The third transcription factor studied, also involved in the regulation of lipogenesis, was
328 PPARgamma. It has been shown that in animal models of IR, PPARgamma levels are
329 increased, promoting lipid storage (Ables 2012; Kawano and Cohen 2013). In
330 agreement with these data, our results showed increased *Pppargamma* levels in the PH
331 groups, thus highlighting the relationship between liver lipid metabolism and glucose
332 and insulin metabolism. Although only the PHanov phenotype presented signs of IR, by
333 the HOMA-IR index, both PH groups showed increased insulin levels and decreased
334 glucose tolerance by the IPGGT test.

335 In addition to an altered expression of the transcription factors modulating lipogenic
336 genes, we found alterations in the mRNA levels of the genes encoding FAS and SCD1,
337 both enzymes involved in lipogenesis. Both PH groups showed increased levels of *Fas*
338 but only the PHanov group showed altered levels of *Scd1*, the enzyme leading to
339 monounsaturated fatty acids. Thus, although the lipogenic pathway was altered in both
340 PH groups, the PHanov showed a deeper dysregulation of the lipogenesis system.

341 The first limiting factor in lipogenesis is the synthesis of Malonyl-CoA, which is
342 synthesized by ACC, which is present in both isoforms encoded by the *Acaca* and
343 *Acacb* genes. Our results surprisingly showed that both mRNA levels were decreased in
344 the PH groups, independently of the increased levels of *Srebp*, *Chrebp* and *Ppargamma*.
345 Malonyl-CoA is an indirect inhibitor of fatty acid oxidation (Browning and Horton
346 2004) and it has been described that when one of the ACC isoforms is reduced, fatty
347 acid oxidation results increased. These findings suggest that the reduction of *Acaca* and
348 *Acacb* expression could be due to the effect of other regulatory mechanisms
349 (independently of *Ppargamma*, *Srebp* and *Chrebp* action), which may be preventing
350 lipid accumulation by decreasing Malonyl-CoA synthesis (Savage, et al. 2006; Strable
351 and Ntambi 2010), thus favoring fatty acid oxidation.

352 Our results are in accordance with other studies (Mao, et al. 2006; Strable and Ntambi
353 2010) that show that *Acaca* levels are independent of the expression of the genes
354 involved in fatty acid synthesis. In fact, the knock-out of *Acaca* shows increased levels
355 of several genes that encode proteins involved in lipogenesis but without hepatic lipid
356 accumulation (Mao, et al. 2006; Strable and Ntambi 2010). These data demonstrate that
357 *Acaca* could be playing a protective role in the development of hepatic steatosis.

358 In addition to the alterations found in the lipogenesis pathways, we found derangements
359 in fatty acid oxidation (Fig. 7). By having opposite functions, *Pparalpha* and
360 *Ppargamma* regulate fat metabolism and while *Ppargamma* promotes lipid storage,
361 *Pparalpha* promotes lipid utilization (Ables 2012; Kawano and Cohen 2013; Souza-
362 Mello 2015). In the present study, prenatal hyperandrogenization decreased *Pparalpha*
363 levels in the liver of PHanov animals, suggesting that this group could be more sensitive
364 to hepatic steatosis. We also found that the levels of the PPARs coactivator, *Pgc1a*, a
365 key regulator of lipid metabolism, were decreased in both PH groups as compared with
366 the control group. In fact, PGC1a not only acts as a regulator of PPARs but also
367 promotes oxidation of fatty acids by binding to specific transcription factors, modulates
368 mitochondrial functions, and controls glucose homeostasis (Fernandez-Marcos and
369 Auwerx 2011; Liang and Ward 2006). Taken together, our data suggest that
370 dysregulation of lipogenesis and fatty acid oxidation could lead in the long-term to the
371 development of hepatic damage, deepened by decreased insulin sensitivity.

372 Oxidative stress and the pro-inflammatory process are also involved in the pathogenesis
373 of hepatic damage. Oxidative stress is involved in the regulation of very low-density
374 lipoprotein (VLDL) production and its excretion by the liver (Pan, et al. 2004).
375 Moreover, the addition of GSH to rat hepatoma cells reverses steatosis and decreases
376 lipid peroxidation levels (Pan et al. 2004). In the liver, GSH levels correlate with high
377 levels of circulating LDL cholesterol, which reinforces the association between the
378 oxidative balance and lipid metabolism (Lin et al. 2014). In agreement with these
379 findings, here we found that GSH compensated the damage caused by lipid peroxidation
380 in the PHov group but not in the PHanov group. We suggest that in the PHov group
381 GSH could be modulating VLDL secretion from the liver to the circulation, as

382 manifested by the increased levels of serum LDL observed, and thus preventing the
383 accumulation of VLDL, as evidenced by the lack of accumulation of lipid droplets.

384 As mentioned before, the pro-inflammatory process is involved in the development of
385 NAFLD (Day and James 1998) and prostaglandins and COX2 play a role in lipid
386 metabolism and lipid accumulation in the liver (Hsieh, et al. 2009; Ii, et al. 2009; Yu, et
387 al. 2006). Increased levels of PGE correlate with TG accumulation in the liver (Henkel,
388 et al. 2012; Hsieh et al. 2009; Ii et al. 2009). In agreement with these data, we found that
389 decreased levels of PGE and COX2 in the PH groups evidenced an alteration in the pro-
390 inflammatory mediators that could be preventing liver fat accumulation. In fact, the
391 decrease in the inflammatory pathway in the PH groups correlated with a lack of
392 increase in TG content. These results contribute to the explanation of the absence of
393 lipid droplets in the PHanov group. Although the liver PPAR system was altered and
394 lipogenesis was favored, there was a systemic manifestation of these consequences seen
395 by an altered circulating lipid profile. Thus, a depletion of the pro-inflammatory
396 mediators could be acting as a compensatory system.

397 Hepatic transaminases have been described as markers of liver function and damage
398 (Vassilatou 2014). Although ALT is one of the hepatic enzymes most used as a marker
399 to detect hepatic injury, several studies have shown other causes for its increase,
400 including growth spurs and looming diabetes (Burgert, et al. 2006; Vassilatou 2014).
401 Despite these findings, it remains controversial whether ALT is a good marker for liver
402 function because some individuals have NAFLD but normal ALT levels and vice versa
403 (Kim, et al. 2008). It has been recommended that increased levels of these enzymes in
404 blood may only be used to detect the inflammation that occurs on the liver due to injury
405 or damage. Unexpectedly, we found increased levels of ALT only in PHov animals.

406 Thus, as the PHanov group presented a great depletion of the pro-inflammatory status,
407 then ALT serum levels would not be affected in these animals (Burgert et al. 2006;
408 Kerner, et al. 2005; Yamada, et al. 2006).

409 It should be pointed out that the incidence of NAFLD and liver fat accumulation are
410 associated with increasing age and body weight (Michaliszyn, et al. 2013; Park, et al.
411 2014). Here, we found no alterations in body weight or fatty liver presence related to the
412 decreased liver inflammation. However, studies are being carried out in adult rats, as we
413 found that derangements in the metabolic pathway of lipogenesis could worsen through
414 life (Heber et al. 2013).

415 Women with the more severe PCOS phenotype show increased prevalence of NAFLD
416 (Jones, et al. 2012). Here we found that the PHanov group was the most affected,
417 displaying decreased expression of *Pgc1a* and *Pparalpha* and over-expression of
418 *Ppargamma*, *Srebp*, *Chrebp*, thus being more susceptible to presenting signs of hepatic
419 steatosis and damage in the long-term (Browning and Horton 2004; Estall, et al. 2009).

420 Our data are in accordance to the multiple hits hypothesis (Day and James 1998; Lin et
421 al. 2014) to explain the origins of NAFLD. This involves IR, fatty acid signaling
422 impairment, oxidative stress and inflammation as contributing factors to NAFLD
423 development. As we found no lipid accumulation but alterations in the processes
424 described, steatosis may be a consequence of hepatic signaling derangements and
425 systemic metabolic detriment. We do not discard that the hepatic alterations found could
426 be due to an increased testosterone/estradiol ratio, worsened in the PHanov group.

427 In summary, our data show for the first time that both ovulatory and anovulatory
428 phenotypes that mimics PCOS features present, at pubertal age, signs of incipient liver
429 injury and an imbalance of the fatty acid metabolism mediated by the PPAR system,

430 SREBP and CHREBP as well as an imbalance of the lipogenic enzymes but without
431 development of NAFLD. These derangements are related to systemic effects,
432 dyslipidemia and decreased glucose tolerance.

433 **Declaration of interests**

434 The authors declare that there is no conflict of interest that could be perceived as
435 prejudicing the impartiality of the research reported.

436 **Funding**

437 This study was supported by grants from Agencia Nacional de Promoción Científica y
438 Tecnológica (ANPCyT) (Grant PICT 577/2012 and PICT 689/2013), Argentina.
439 G.A.A., M.F.H, L.M.V. are supported by a doctoral fellowship awarded by CONICET
440 and. S.R.F. by ANPCyT. O. P.P. and A.B.M. are PhD from CONICET.

441 **Author contributions**

442 Conceived and designed the experiments AMB, GAA and MFH. Performed the
443 experiments: GAA, MFH, SRF, LMV, RR and OPP. Analyzed the data: GAA and
444 MFH. Contributed reagents/materials/analysis tools: GAA, MFH, SRF, LMV, OPP,
445 ABM. Wrote the paper: GAA and ABM. Corrected and read the last version: GAA,
446 MFH, SRF, LMV, RR, OPP and ABM.

447 **Acknowledgements**

448 We thank Enzo Cuba and Marcela Marquez for their technical support in the animal
449 care and Dr. Gladys Hermida for her support with histological techniques.

450 **References**

451 Abbott DH, Barnett DK, Bruns CM & Dumesic DA 2005 Androgen excess fetal programming
452 of female reproduction: a developmental aetiology for polycystic ovary syndrome? *Hum Reprod*
453 *Update* **11** 357-374.

- 454 Abbott DH, Bruns CR, Barnett DK, Dunaif A, Goodfriend TL, Dumesic DA & Tarantal AF
455 2010 Experimentally induced gestational androgen excess disrupts glucoregulation in rhesus
456 monkey dams and their female offspring. *Am J Physiol Endocrinol Metab* **299** E741-751.
- 457 Ables GP 2012 Update on Ppar. *PPAR Research* **2012** 5.
- 458 Amalfi S, Velez LM, Heber MF, Vighi S, Ferreira SR, Orozco AV, Pignataro O & Motta AB
459 2012 Prenatal hyperandrogenization induces metabolic and endocrine alterations which depend
460 on the levels of testosterone exposure. *PLoS One* **7** e37658.
- 461 Baranova A, Tran TP, Afendy A, Wang L, Shamsaddini A, Mehta R, Chandhoke V, Birerdinc
462 A & Younossi ZM 2013 Molecular signature of adipose tissue in patients with both non-
463 alcoholic fatty liver disease (NAFLD) and polycystic ovarian syndrome (PCOS). *J Transl Med*
464 **11** 133.
- 465 Baranova A, Tran TP, Birerdinc A & Younossi ZM 2011 Systematic review: association of
466 polycystic ovary syndrome with metabolic syndrome and non-alcoholic fatty liver disease.
467 *Aliment Pharmacol Ther* **33** 801-814.
- 468 Browning JD & Horton JD 2004 Molecular mediators of hepatic steatosis and liver injury. *J*
469 *Clin Invest* **114** 147-152.
- 470 Brumbaugh DE & Friedman JE 2014 Developmental origins of nonalcoholic fatty liver disease.
471 *Pediatr Res* **75** 140-147.
- 472 Burgert TS, Taksali SE, Dziura J, Goodman TR, Yeckel CW, Papademetris X, Constable RT,
473 Weiss R, Tamborlane WV, Savoye M, et al. 2006 Alanine aminotransferase levels and fatty
474 liver in childhood obesity: associations with insulin resistance, adiponectin, and visceral fat. *J*
475 *Clin Endocrinol Metab* **91** 4287-4294.
- 476 Chow JD, Jones ME, Prella K, Simpson ER & Boon WC 2011 A selective estrogen receptor
477 alpha agonist ameliorates hepatic steatosis in the male aromatase knockout mouse. *J Endocrinol*
478 **210** 323-334.
- 479 Day CP & James OF 1998 Steatohepatitis: a tale of two "hits"? *Gastroenterology* **114** 842-845.
- 480 Demissie M, Lasic M, Foecking EM, Aird F, Dunaif A & Levine JE 2008 Transient prenatal
481 androgen exposure produces metabolic syndrome in adult female rats. *Am J Physiol Endocrinol*
482 *Metab* **295** E262-268.
- 483 den Boer M, Voshol PJ, Kuipers F, Havekes LM & Romijn JA 2004 Hepatic steatosis: a
484 mediator of the metabolic syndrome. Lessons from animal models. *Arterioscler Thromb Vasc*
485 *Biol* **24** 644-649.
- 486 Estall JL, Kahn M, Cooper MP, Fisher FM, Wu MK, Laznik D, Qu L, Cohen DE, Shulman GI
487 & Spiegelman BM 2009 Sensitivity of lipid metabolism and insulin signaling to genetic
488 alterations in hepatic peroxisome proliferator-activated receptor-gamma coactivator-1alpha
489 expression. *Diabetes* **58** 1499-1508.
- 490 Fernandez-Marcos PJ & Auwerx J 2011 Regulation of PGC-1alpha, a nodal regulator of
491 mitochondrial biogenesis. *Am J Clin Nutr* **93** 884S-890.

- 492 Foecking EM, McDevitt MA, Acosta-Martinez M, Horton TH & Levine JE 2008
493 Neuroendocrine consequences of androgen excess in female rodents. *Horm Behav* **53** 673-692.
- 494 Franks S 1995 Polycystic ovary syndrome. *N Engl J Med* **333** 853-861.
- 495 Franks S 2003 Assessment and management of anovulatory infertility in polycystic ovary
496 syndrome. *Endocrinol Metab Clin North Am* **32** 639-651.
- 497 Franks S & Berga SL 2012 Does PCOS have developmental origins? *Fertility and Sterility* **97**
498 2-6.
- 499 Gambarin-Gelwan M, Kinkhabwala SV, Schiano TD, Bodian C, Yeh HC & Futterweit W 2007
500 Prevalence of nonalcoholic fatty liver disease in women with polycystic ovary syndrome. *Clin*
501 *Gastroenterol Hepatol* **5** 496-501.
- 502 Gluckman PD & Hanson MA 2004 Developmental origins of disease paradigm: a mechanistic
503 and evolutionary perspective. *Pediatric Research* **56** 311-317.
- 504 Heber MF, Ferreira SR, Velez LM & Motta AB 2013 Prenatal hyperandrogenism and lipid
505 profile during different age stages: an experimental study. *Fertil Steril* **99** 551-557.
- 506 Henkel J, Frede K, Schanze N, Vogel H, Schurmann A, Spruss A, Bergheim I & Puschel GP
507 2012 Stimulation of fat accumulation in hepatocytes by PGE(2)-dependent repression of hepatic
508 lipolysis, beta-oxidation and VLDL-synthesis. *Lab Invest* **92** 1597-1606.
- 509 Hogg K, Wood C, McNeilly AS & Duncan WC 2011 The in utero programming effect of
510 increased maternal androgens and a direct fetal intervention on liver and metabolic function in
511 adult sheep. *PLoS One* **6** e24877.
- 512 Hsieh PS, Jin JS, Chiang CF, Chan PC, Chen CH & Shih KC 2009 COX-2-mediated
513 inflammation in fat is crucial for obesity-linked insulin resistance and fatty liver. *Obesity (Silver*
514 *Spring)* **17** 1150-1157.
- 515 Ii H, Yokoyama N, Yoshida S, Tsutsumi K, Hatakeyama S, Sato T, Ishihara K & Akiba S 2009
516 Alleviation of high-fat diet-induced fatty liver damage in group IVA phospholipase A2-
517 knockout mice. *PLoS One* **4** e8089.
- 518 Jang H, Bhasin S, Guarneri T, Serra C, Schneider M, Lee MJ, Guo W, Fried SK, Pencina K &
519 Jasuja R 2015 The Effects of a Single Developmentally Entrained Pulse of Testosterone in
520 Female Neonatal Mice on Reproductive and Metabolic Functions in Adult Life. *Endocrinology*
521 **156** 3737-3746.
- 522 Jonard S & Dewailly D 2004 The follicular excess in polycystic ovaries, due to intra-ovarian
523 hyperandrogenism, may be the main culprit for the follicular arrest. *Hum Reprod Update* **10**
524 107-117.
- 525 Jones H, Sprung VS, Pugh CJ, Daousi C, Irwin A, Aziz N, Adams VL, Thomas EL, Bell JD,
526 Kemp GJ, et al. 2012 Polycystic ovary syndrome with hyperandrogenism is characterized by an
527 increased risk of hepatic steatosis compared to nonhyperandrogenic PCOS phenotypes and
528 healthy controls, independent of obesity and insulin resistance. *J Clin Endocrinol Metab* **97**
529 3709-3716.

- 530 Karim BO, Landolfi JA, Christian A, Ricart-Arbona R, Qiu W, McAlonis M, Eyabi PO, Khan
531 KA, Dicello JF, Mann JF, et al. 2003 Estrous cycle and ovarian changes in a rat mammary
532 carcinogenesis model after irradiation, tamoxifen chemoprevention, and aging. *Comp Med* **53**
533 532-538.
- 534 Kawano Y & Cohen DE 2013 Mechanisms of hepatic triglyceride accumulation in non-
535 alcoholic fatty liver disease. *J Gastroenterol* **48** 434-441.
- 536 Kerner A, Avizohar O, Sella R, Bartha P, Zinder O, Markiewicz W, Levy Y, Brook GJ &
537 Aronson D 2005 Association between elevated liver enzymes and C-reactive protein: possible
538 hepatic contribution to systemic inflammation in the metabolic syndrome. *Arterioscler Thromb*
539 *Vasc Biol* **25** 193-197.
- 540 Kim WR, Flamm SL, Di Bisceglie AM, Bodenheimer HC & Public Policy Committee of the
541 American Association for the Study of Liver D 2008 Serum activity of alanine aminotransferase
542 (ALT) as an indicator of health and disease. *Hepatology* **47** 1363-1370.
- 543 Lee JH, Friso S & Choi SW 2014 Epigenetic mechanisms underlying the link between non-
544 alcoholic fatty liver diseases and nutrition. *Nutrients* **6** 3303-3325.
- 545 Liang H & Ward WF 2006 PGC-1alpha: a key regulator of energy metabolism. *Adv Physiol*
546 *Educ* **30** 145-151.
- 547 Lin Z, Cai F, Lin N, Ye J, Zheng Q & Ding G 2014 Effects of glutamine on oxidative stress and
548 nuclear factor-kappaB expression in the livers of rats with nonalcoholic fatty liver disease. *Exp*
549 *Ther Med* **7** 365-370.
- 550 Madan K, Bhardwaj P, Thareja S, Gupta SD & Saraya A 2006 Oxidant stress and antioxidant
551 status among patients with nonalcoholic fatty liver disease (NAFLD). *J Clin Gastroenterol* **40**
552 930-935.
- 553 Manikkam M, Steckler TL, Welch KB, Inskeep EK & Padmanabhan V 2006 Fetal
554 programming: prenatal testosterone treatment leads to follicular persistence/luteal defects;
555 partial restoration of ovarian function by cyclic progesterone treatment. *Endocrinology* **147**
556 1997-2007.
- 557 Mao J, DeMayo FJ, Li H, Abu-Elheiga L, Gu Z, Shaikenov TE, Kordari P, Chirala SS, Heird
558 WC & Wakil SJ 2006 Liver-specific deletion of acetyl-CoA carboxylase 1 reduces hepatic
559 triglyceride accumulation without affecting glucose homeostasis. *Proc Natl Acad Sci U S A* **103**
560 8552-8557.
- 561 Michaliszyn SF, Lee S, Tfayli H & Arslanian S 2013 Polycystic ovary syndrome and
562 nonalcoholic fatty liver in obese adolescents: association with metabolic risk profile. *Fertil*
563 *Steril* **100** 1745-1751.
- 564 Motta AB, Estevez A & de Gimeno MF 1999 The involvement of nitric oxide in corpus luteum
565 regression in the rat: feedback mechanism between prostaglandin F(2alpha) and nitric oxide.
566 *Mol Hum Reprod* **5** 1011-1016.
- 567 Pan M, Cederbaum AI, Zhang YL, Ginsberg HN, Williams KJ & Fisher EA 2004 Lipid
568 peroxidation and oxidant stress regulate hepatic apolipoprotein B degradation and VLDL
569 production. *J Clin Invest* **113** 1277-1287.

- 570 Park JH, Kim SH, Park S & Park MJ 2014 Alanine aminotransferase and metabolic syndrome in
571 adolescents: the Korean National Health and Nutrition Examination Survey Study. *Pediatr Obes*
572 **9** 411-418.
- 573 Paschos P & Paletas K 2009 Non alcoholic fatty liver disease and metabolic syndrome.
574 *Hippokratia* **13** 9-19.
- 575 Regueira E, Davila C & Hermida GN 2016 Morphological Changes in Skin Glands During
576 Development in *Rhinella Arenarum* (Anura: Bufonidae). *Anat Rec (Hoboken)* **299** 141-156.
- 577 Rosenfield RL 2007 Does a primary acceleration of LH pulse frequency underlie an association
578 between central precocious puberty and polycystic ovary syndrome? Commentary on Escobar
579 ME et al: Acceleration of LH pulse frequency in adolescent girls with a history of central
580 precocious puberty with versus without hyperandrogenism (*Horm Res* 2007;68:278-285). *Horm*
581 *Res* **68** 286-287.
- 582 Savage DB, Choi CS, Samuel VT, Liu ZX, Zhang D, Wang A, Zhang XM, Cline GW, Yu XX,
583 Geisler JG, et al. 2006 Reversal of diet-induced hepatic steatosis and hepatic insulin resistance
584 by antisense oligonucleotide inhibitors of acetyl-CoA carboxylases 1 and 2. *J Clin Invest* **116**
585 817-824.
- 586 Schwimmer JB, Khorram O, Chiu V & Schwimmer WB 2005 Abnormal aminotransferase
587 activity in women with polycystic ovary syndrome. *Fertil Steril* **83** 494-497.
- 588 Souza-Mello V 2015 Peroxisome proliferator-activated receptors as targets to treat non-
589 alcoholic fatty liver disease. *World J Hepatol* **7** 1012-1019.
- 590 Strable MS & Ntambi JM 2010 Genetic control of de novo lipogenesis: role in diet-induced
591 obesity. *Crit Rev Biochem Mol Biol* **45** 199-214.
- 592 Vassilatou E 2014 Nonalcoholic fatty liver disease and polycystic ovary syndrome. *World J*
593 *Gastroenterol* **20** 8351-8363.
- 594 Vassilatou E, Lafoyianni S, Vryonidou A, Ioannidis D, Kosma L, Katsoulis K, Papavassiliou E
595 & Tzavara I 2010 Increased androgen bioavailability is associated with non-alcoholic fatty liver
596 disease in women with polycystic ovary syndrome. *Hum Reprod* **25** 212-220.
- 597 Wolf CJ, Hotchkiss A, Ostby JS, LeBlanc GA & Gray LE, Jr. 2002 Effects of prenatal
598 testosterone propionate on the sexual development of male and female rats: a dose-response
599 study. *Toxicol Sci* **65** 71-86.
- 600 Woodruff TK, Lyon RJ, Hansen SE, Rice GC & Mather JP 1990 Inhibin and activin locally
601 regulate rat ovarian folliculogenesis. *Endocrinology* **127** 3196-3205.
- 602 Yamada J, Tomiyama H, Yambe M, Koji Y, Motobe K, Shiina K, Yamamoto Y & Yamashina
603 A 2006 Elevated serum levels of alanine aminotransferase and gamma glutamyltransferase are
604 markers of inflammation and oxidative stress independent of the metabolic syndrome.
605 *Atherosclerosis* **189** 198-205.
- 606 Yan X, Dai X, Wang J, Zhao N, Cui Y & Liu J 2013 Prenatal androgen excess programs
607 metabolic derangements in pubertal female rats. *J Endocrinol* **217** 119-129.

- 608 Yasui K, Hashimoto E, Tokushige K, Koike K, Shima T, Kanbara Y, Saibara T, Uto H, Takami
609 S, Kawanaka M, et al. 2012 Clinical and pathological progression of non-alcoholic
610 steatohepatitis to hepatocellular carcinoma. *Hepatol Res* **42** 767-773.
- 611 Yu J, Ip E, Dela Pena A, Hou JY, Sessa J, Pera N, Hall P, Kirsch R, Leclercq I & Farrell GC
612 2006 COX-2 induction in mice with experimental nutritional steatohepatitis: Role as pro-
613 inflammatory mediator. *Hepatology* **43** 826-836.
- 614

Legends of figures

Figure 1. Prenatally hyperandrogenized murine model. Prenatal hyperandrogenism in female offspring of control (Ctl) and prenatally hyperandrogenized (PH) groups. **(A)** Serum testosterone levels. Each column represents the mean \pm SEM from fifteen different animals per group, a vs b $p < 0.01$ by ANOVA test. **(B)** Serum estradiol levels. Each column represents the mean \pm SEM from fifteen different animals per group, a vs b $p < 0.05$ by ANOVA test. **(C)** A representative ovarian tissue section from the Ctl group (40X). **(D)** A representative ovarian tissue section from the PHov group (40X). **(E)** A representative ovarian tissue section from the PHanov group (40X). **(F)** Detail of a representative ovarian cyst from the PH groups (100X). Corpus luteum (CL), antral follicle (AF), cyst (Cy), granulosa cells (GC), theca cells (ThC) and preantral follicles (PaF).

Figure 2. Effects of prenatal hyperandrogenism on liver transaminase levels and lipid content. **(A)** Serum levels of ALT and **(B)** AST. **(C)** GGT. Each column represents the mean \pm SEM of control (Ctl) and prenatally hyperandrogenized (PH) groups; a vs b $p < 0.05$, by ANOVA test. Liver lipid content was quantified by SUDAN IV staining. **(D)** The cytoplasmic lipid droplets are shown in red, as shown in the positive control of the technique (arrows). Each photo shows the detail (100X) of a representative staining of the Ctl group **(E)** and PHov **(F)** and PHanov groups **(G)**. There was no evidence of cytoplasmic lipid accumulation. **(H)** TG content in the liver. No significant differences were found between the Ctl and PH groups ($p > 0.05$, by ANOVA test).

Figure 3. Effects of prenatal hyperandrogenism on liver lipid metabolism

The graphs correspond to the mRNA abundance of the gene of interest relative to *L32* mRNA levels of control (Ctl) and prenatally hyperandrogenized (PH) groups. *L32* was validated as a reference gene using Cts (cycle threshold) (Control=21.76 + 0.24; PHov=21.36 + 0.30; PHanov= 21.70 + 0.34; p=0.67) (A) Gene expression of *Ppargamma* (a vs b p<0.01), (B) *Srebp* (a vs b p<0.05) (C) *Chrebp* (a vs b p<0.05), (D) *Acaca* (a vs b p<0.01), (E) *Acacb* (a vs b p<0.01), (F) *Fas* (a vs b p<0.01), (G) *Scd1* (a vs b p<0.05), (H) *Pparalpha* (a vs b p<0.01), and (I) *Pgc1a* (a vs b p<0.01). Each column represents the mean \pm SEM. Statistical analyses were made by ANOVA test.

Figure 4. Effects of prenatal hyperandrogenism on liver oxidant/antioxidant balance and proinflammatory status. The oxidant–antioxidant balance in liver tissue was evaluated by measuring the lipid peroxidation index (A) and the content of the antioxidant glutathione (B). Each column represents the mean \pm SEM. Different letters mean statistical significant differences (a#b#c, p<0.05 in both cases, by ANOVA test). (C) Liver PGE content was measured to evaluate the pro-inflammatory status (a#b#c, p<0.01 by ANOVA). (D) To evaluate whether PGE levels were influenced by the limiting enzyme of its synthesis, COX2 was measured, a vs b p<0.05, by ANOVA test. Each column represents the mean \pm SEM.

Figure 5. Prenatal hyperandrogenism and metabolic derangements. Metabolic features evaluated in female offspring of control (Ctl) and prenatally hyperandrogenized (PH) groups. (A) The curve represents the mean growth rates of the Ctl and PH groups. Differences between growth rates were not significant (p>0.05, by ANOVA test). (B) Basal insulin levels, a vs b p<0.05. (C) Basal glucose levels a vs b p<0.05. (D) Blood samples followed by intraperitoneal injection of 2 g dextrose/kg body weight were

collected at 0, 30, 60, 90 and 120 minutes post-injection for IPGTT. (E) HOMA-IR index a vs b $p < 0.05$. Values are mean \pm SEM by ANOVA test.

Figure 6. Effect of prenatal hyperandrogenism on the circulating lipid profile. (A) Serum levels of low-density lipoprotein cholesterol (LDL-cholesterol), (B) triglycerides, (C) total cholesterol and (D) high-density lipoprotein cholesterol (HDL-cholesterol). Each column represents the mean + SEM of control (Ctl) and prenatally hyperandrogenized (PH) groups; a vs b $p < 0.01$ panel A; $p < 0.05$ panel B. Data were analyzed by ANOVA test.

Figure 7. Mediators of hepatic lipogenesis and β -oxidation. SREBP, ChREBP and PPARgamma are transcription factors involved in the regulation of hepatic lipogenesis. Insulin and glucose modulate SREBP and ChREBP, respectively. These transcription factors and PPARgamma positively regulate *de novo* lipogenesis by modulating the expression of the enzymes involved in this pathway. On the other hand, PPARalpha and PGC1a are positively regulators of genes involved in fatty acid oxidation. A balance between these processes is needed to avoid hepatic liver accumulation leading to steatosis. Insulin resistance is associated with an increase in lipogenesis due to an up-regulation of ChREBP, SREBP-1c and PPARgamma and a decrease in fatty acid oxidation due to a negative regulation on PPARalpha.

Primers used in real-time PCR

Gene	Primers sequences	Temperature of melting(°C)
<i>Ppargamma</i> F	5'-TTTTCAAGGGTGCCAGTTTC-3'	60
<i>Ppargamma</i> R	5'-GAGGCCAGCATGGTGTAGAT-3'	
<i>Srebp</i> F	5'- TAACCTGGCTGAGTGTGCAG -3'	60
<i>Srebp</i> R	5'- ATCCACGAAGAAACGGTGAC -3'	
<i>Chrebp</i> F	5'- GGTTGTCCCAAAGCAGAGA -3'	62
<i>Chrebp</i> R	5'- TTGTTGTCTACACGACCCCG -3'	
<i>Acaca</i> F	5'-CCAGACCCTTTCTTCAGCAG-3'	62
<i>Acaca</i> R	5'-AGGACCGATGTGATGTTGCT-3'	
<i>Acacb</i> F	5'-CAAAGCCTCTGAAGGTGGAG-3'	62
<i>Acacb</i> R	5'- CTCGTCCAAACAGGGACACT -3'	
<i>Fas</i> F	5'-TCGAGACACATCGTTTGAGC-3'	62
<i>Fas</i> R	5'-CCCAGAGGGTGGTTGTTAGA-3'	
<i>Scd1</i> F	5'-GCTTCCAGATCCTCCCTACC-3'	62
<i>Scd1</i> R	5'-CAACAACCAACCCTCTCGTT-3'	
<i>Pparalpha</i> F	5'-TCACACGATGCAATCCGTTT-3'	60
<i>Pparalpha</i> R	5'-GGCCTTGACCTTGTTTCATGT-3'	
<i>Pgc1a</i> F	5'-AATGCAGCGGTCTTAGCACT-3'	60
<i>Pgc1a</i> R	5'-GTGTGAGGAGGGTCATCGTT-3'	
<i>L32</i> F	5'-TGGTCCACAATGTCAAGG-3'	58
<i>L32</i> R	5'-CAAAACAGGCACACAAGC-3'	

Table 1 :List of primers used in real-time PCR. (F) forward sequence, (R) reverse sequence.

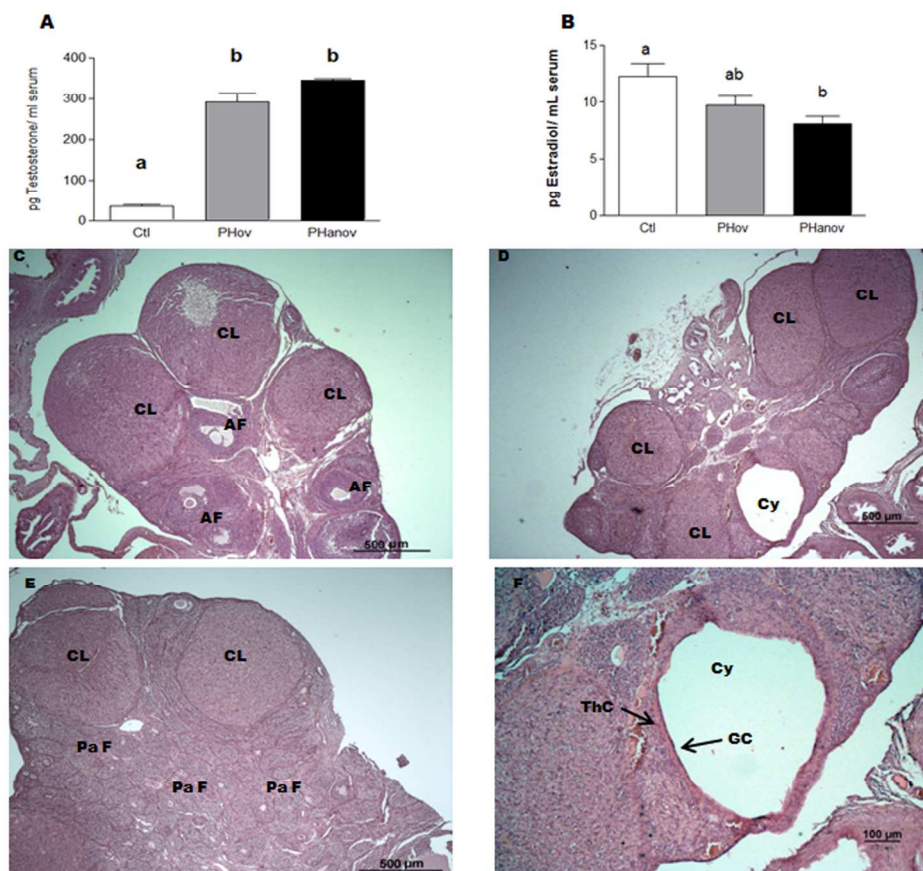
Figure 1

Figure 1. Prenatally hyperandrogenized murine model. Prenatal hyperandrogenism in female offspring of control (Ctl) and prenatally hyperandrogenized (PH) groups. (A) Serum testosterone levels. Each column represents the mean + SEM from fifteen different animals per group, a vs b $p < 0.01$ by ANOVA test. (B) Serum estradiol levels. Each column represents the mean + SEM from fifteen different animals per group, a vs b $p < 0.05$ by ANOVA test. (C) A representative ovarian tissue section from the Ctl group (40X). (D) A representative ovarian tissue section from the PHov group (40X). (E) A representative ovarian tissue section from the PHanov group (40X). (F) Detail of a representative ovarian cyst from the PH groups (100X). Corpus luteum (CL), antral follicle (AF), cyst (Cy), granulosa cells (GC), theca cells (ThC) and preantral follicles (PaF).

194x190mm (300 x 300 DPI)

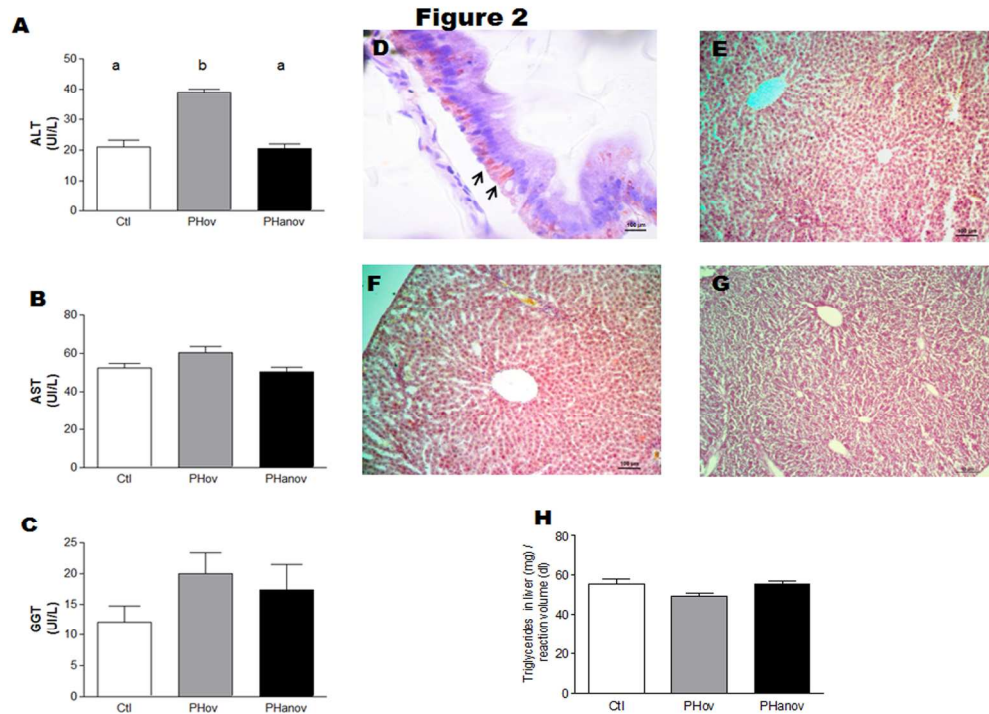
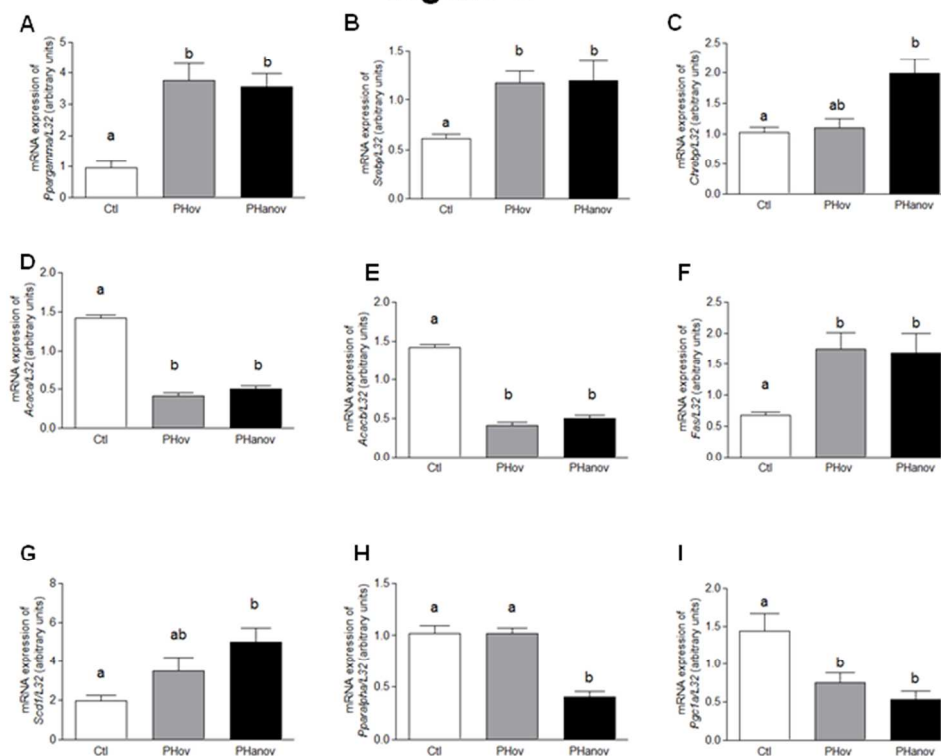


Figure 2. Effects of prenatal hyperandrogenism on liver transaminase levels and lipid content. (A) Serum levels of ALT and (B) AST. (C) GGT. Each column represents the mean + SEM of control (Ctl) and prenatally hyperandrogenized (PH) groups; a vs b $p < 0.05$, by ANOVA test. Liver lipid content was quantified by SUDAN IV staining. (D) The cytoplasmic lipid droplets are shown in red, as shown in the positive control of the technique (arrows). Each photo shows the detail (100X) of a representative staining of the Ctl group (E) and PHov (F) and PHanov groups (G). There was no evidence of cytoplasmic lipid accumulation. (H) TG content in the liver. No significant differences were found between the Ctl and PH groups ($p > 0.05$, by ANOVA test).

254x190mm (300 x 300 DPI)

Figure 3**Figure 3. Effects of prenatal hyperandrogenism on liver lipid metabolism**

The graphs correspond to the mRNA abundance of the gene of interest relative to L32 mRNA levels of control (Ctl) and prenatally hyperandrogenized (PH) groups. L32 was validated as a reference gene using Cts (cycle threshold) (Control=21.76 + 0.24; PHov= 21.36 + 0.30; PHanov= 21.70 + 0.34; p=0.67) (A) Gene expression of Ppargamma (a vs b p<0.01), (B) Srebp (a vs b p<0.05) (C) Chrebp (a vs b p<0.05), (D) Acaca (a vs b p<0.01), (E) Acacb (a vs b p<0.01), (F) Fas (a vs b p<0.01), (G) Scd1 (a vs b p<0.05), (H) Pparalpha (a vs b p<0.01), and (I) Pgc1a (a vs b p<0.01). Each column represents the mean + SEM. Statistical analyses were made by ANOVA test.

254x228mm (300 x 300 DPI)

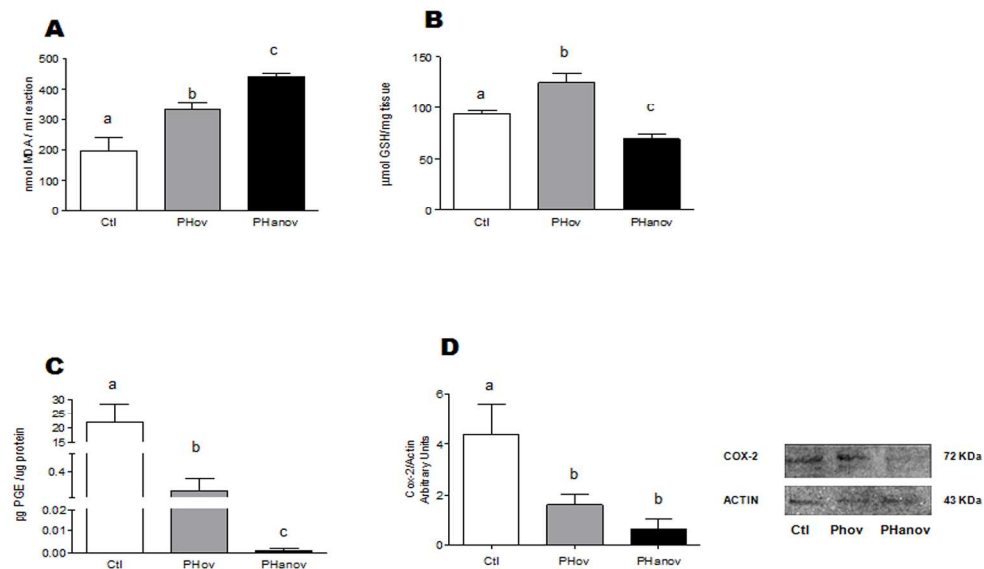
Figure 4

Figure 4. Effects of prenatal hyperandrogenism on liver oxidant/antioxidant balance and proinflammatory status. The oxidant–antioxidant balance in liver tissue was evaluated by measuring the lipid peroxidation index (A) and the content of the antioxidant glutathione (B). Each column represents the mean + SEM. Different letters mean statistical significant differences ($a \neq b \neq c$, $p < 0.05$ in both cases, by ANOVA test). (C) Liver PGE content was measured to evaluate the pro-inflammatory status ($a \neq b \neq c$, $p < 0.01$ by ANOVA). (D) To evaluate whether PGE levels were influenced by the limiting enzyme of its synthesis, COX2 was measured, a vs b $p < 0.05$, by ANOVA test. Each column represents the mean + SEM.

288x207mm (300 x 300 DPI)

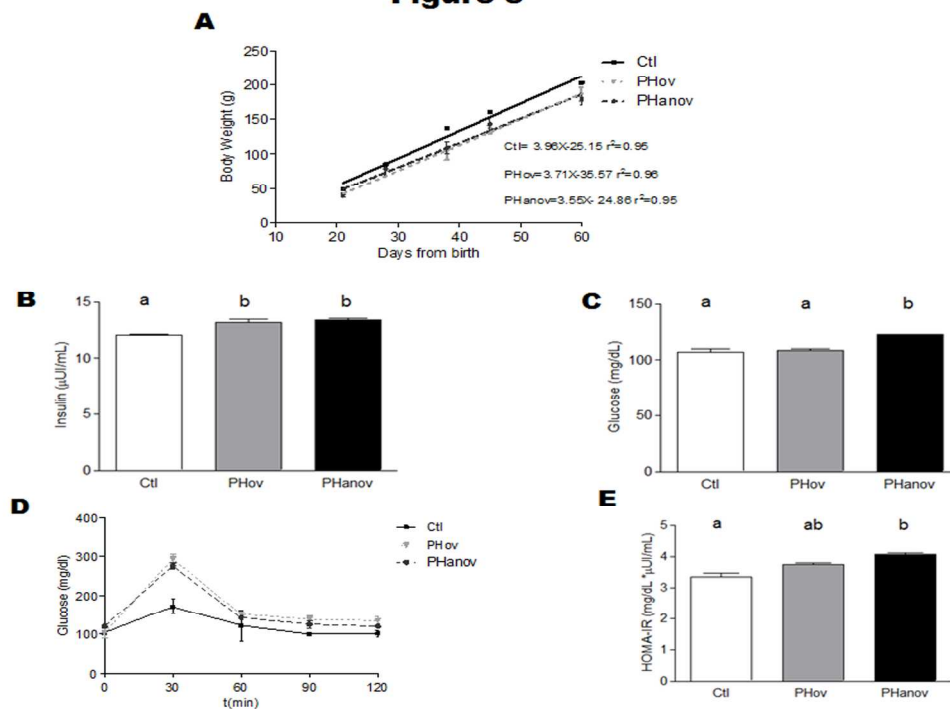
Figure 5

Figure 5. Prenatal hyperandrogenism and metabolic derangements. Metabolic features evaluated in female offspring of control (Ctl) and prenatally hyperandrogenized (PH) groups. (A) The curve represents the mean growth rates of the Ctl and PH groups. Differences between growth rates were not significant ($p > 0.05$, by ANOVA test). (B) Basal insulin levels, a vs b $p < 0.05$. (C) Basal glucose levels a vs b $p < 0.05$. (D) Blood samples followed by intraperitoneal injection of 2 g dextrose/kg body weight were collected at 0, 30, 60, 90 and 120 minutes post-injection for IPGTT. (E) HOMA-IR index a vs b $p < 0.05$. Values are mean + SEM by ANOVA test.

254x190mm (300 x 300 DPI)

Figure 6

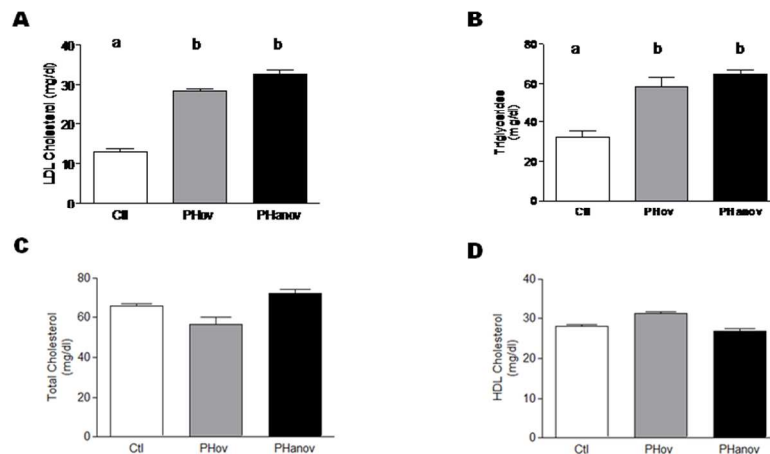


Figure 6. Effect of prenatal hyperandrogenism on the circulating lipid profile. (A) Serum levels of low-density lipoprotein cholesterol (LDL-cholesterol), (B) triglycerides, (C) total cholesterol and (D) high-density lipoprotein cholesterol (HDL-cholesterol). Each column represents the mean + SEM of control (Ctl) and prenatally hyperandrogenized (PH) groups; a vs b $p < 0.01$ panel A; $p < 0.05$ panel B. Data were analyzed by ANOVA test.

254x147mm (300 x 300 DPI)

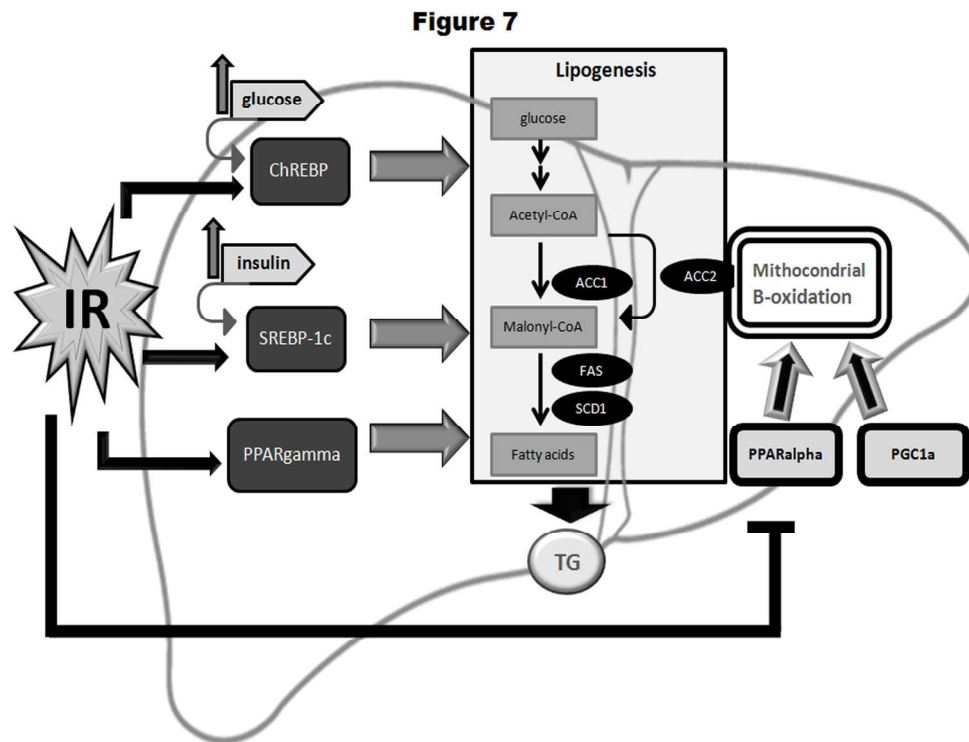


Figure 7. Mediators of hepatic lipogenesis and β -oxidation. SREBP, ChREBP and PPARgamma are transcription factors involved in the regulation of hepatic lipogenesis. Insulin and glucose modulate SREBP and ChREBP, respectively. These transcription factors and PPARgamma positively regulate de novo lipogenesis by modulating the expression of the enzymes involved in this pathway. On the other hand, PPARalpha and PGC1a are positive regulators of genes involved in fatty acid oxidation. A balance between these processes is needed to avoid hepatic liver accumulation leading to steatosis. Insulin resistance is associated with an increase in lipogenesis due to an up-regulation of ChREBP, SREBP-1c and PPARgamma and a decrease in fatty acid oxidation due to a negative regulation on PPARalpha.

190x142mm (300 x 300 DPI)